Author(s): Harju, A. & Siljamäki, S. & Nieminen, Risto M.

Title: Wigner molecules in quantum dots: A quantum Monte Carlo study

Year: 2002

Version: Final published version

Please cite the original version:

Harju, A. & Siljamäki, S. & Nieminen, Risto M. 2002. Wigner molecules in quantum dots: A quantum Monte Carlo study. Physical Review B. Volume 65, Issue 7. 075309/1-6. ISSN 1550-235X (electronic). DOI: 10.1103/physrevb.65.075309.

Wigner molecules in quantum dots: A quantum Monte Carlo study

A. Harju, S. Siljamäki, and R. M. Nieminen
Laboratory of Physics, Helsinki University of Technology, P.O. Box 1100, 02015 HUT, Finland
(Received 14 August 2001; published 23 January 2002)

We study two-dimensional quantum dots using the variational quantum Monte Carlo technique in the weak-confinement limit where the system approaches the Wigner molecule, i.e., the classical solution of point charges in an external potential. We observe the spin-polarization of electrons followed by a smooth transition to a Wigner-molecule-like state as the confining potential is made weaker.

DOI: 10.1103/PhysRevB.65.075309 PACS number(s): 73.21.La, 71.10.−w

I. INTRODUCTION

Semiconductor quantum dots (QD's) are small devices containing a tunable number of electrons in an external confinement potential.[1] The significant progress in the fabrication of these devices during the last few years[2] has stimulated an increasing interest in investigating the properties of such systems. From the theoretical point of view, QD's are ideal many-electron objects for the study of fundamental physical properties of correlated electrons.

Perhaps the most striking feature in these artificial atoms is that the system parameters can easily be changed, unlike in real atoms where the parameters are natural constants. Also the typical length scales of interactions and confinement are equal, which should in principle make the correlation effects more enhanced compared to normal atoms. However, the experimentally observed states of QD's in weak magnetic fields can easily be understood as single configurations of noninteracting one-particle states.[2,3] One might suppose that the lack of a strong central Coulomb potential (which organizes the states of normal atoms to shells) would make it more difficult to identify the electronic structure of artificial atoms. It turns out, however, that the important role of the central potential is taken by the symmetries of the many-body wave function.[3,4] Consequently the understanding of the topology of the many-body wave function is of central importance.

A most suitable method for studying the many-body wave functions is the variational quantum Monte Carlo (VMC) technique. It is intimately coupled to the structure of the wave function, and the use of the variational principle enables one to find the best form. The exact diagonalization (ED) method is useful for the studies of small electron numbers[3] or for finding eigenstates in some important subspace of the full Hilbert space, as in the studies of electrons in such a strong magnetic field that the physics is mainly determined by the single-particle states of the lowest Landau level.[4] ED has been used for QD's by many authors, see Ref. 5, and references therein. Mean-field methods such as the spin-density functional theory (SDFT) are especially useful when the number of particles is large.[5]

In this work, we first compare our VMC results with the most accurate energies in the literature, showing that a rather intuitive wave function results in extremely accurate energies. Then we concentrate on the weak confinement limit of a six-electron QD. One should note that making confinement weaker makes the density smaller. In this limit the QD approaches the classical solution of point charges in the QD potential. The most accurate results for this limit are restricted to rather strong confinement,[5] where no trace of Wigner molecule or spin polarization was found. For weaker confinements than considered in Ref. 5 we find that the system spin polarizes before the electrons localize around the classical positions. We also introduce a conditional probability density which shows to be a good measure of the extent of the localization of the electrons. In addition, we find an interesting independent-electron-type scaling of the energy for a large range of confinement strengths.

II. MODEL AND METHOD

The commonly used Hamiltonian for N electrons in a two-dimensional QD can be written as

$$H=\sum_{i=1}^{N}\left(-\frac{\hbar^2}{2m^*}\nabla_i^2+\frac{m^*\omega^2}{2}r_i^2\right)+\sum_{i<j}\frac{e^2}{\epsilon r_{ij}}, \qquad (1)$$

where ω is the strength of the external confining potential, and the effective mass of the electrons m^* and the dielectric constant ϵ are used to model the properties of the semiconductor material studied. For GaAs, the material parameters are $m^*/m_e=0.067$ and $\epsilon=12.4$.[6] We assume that the electrons move in the $z=0$ plane and omit the magnetic field in this study.

In this work, we use variational wave functions of the form

$$\Psi=D_\uparrow D_\downarrow\prod_{i<j}^{N}J(r_{ij}), \qquad (2)$$

where the first two factors are Slater determinants for the two spin types and J is a Jastrow two-body correlation factor. We neglect the three-body and higher correlations. For the Jastrow factor we use

$$J(r)=e^{Cr/(a+br)}, \qquad (3)$$

where a is fixed by the cusp condition to be 3 for a pair of equal spins and 1 for opposite ones and b is a parameter, different for both spin-pair possibilities. We take the wave function to be real, as we have neglected the magnetic field. The single-particle states ψ are expanded in the basis of Gaussians as

$$\psi(\mathbf{r}) = \sum_{i=1}^{N_s} c_i H_{n_{x,i}}(\hat{x}) H_{n_{y,i}}(\hat{y}) e^{-(1/2)\hat{r}^2}, \tag{4}$$

where H_n is a Hermite polynomial of order n and $\hat{\mathbf{r}} = (\hat{x}, \hat{y}) = (c_x x, c_y y)$, where c_x and c_y scale coordinates.

We calculate the energy E which is bound by the exact energy E_0 using

$$E_0 \leqslant E = \lim_{M \to \infty} \frac{1}{M} \sum_{i=1}^{M} E_L(\mathbf{R}_i), \tag{5}$$

where the local energy is $E_L = H\Psi/\Psi$, and depends on the electron configuration **R**. The configurations **R** are distributed according to $|\Psi|^2$. We optimize the variational parameters using the stochastic gradient approximation (SGA).[9] The SGA optimization method involves stochastic simulation in two spaces: the configuration and the parameter space. In the configuration space, a set of m configurations $\{\mathbf{R}_j\}$ is sampled from a distribution $|\Psi(\boldsymbol{\alpha})|^2$, where $\boldsymbol{\alpha}$ is the current parameter vector. In the parameter space, the parameters at iteration $i+1$ are obtained from the previous ones by the formula

$$\boldsymbol{\alpha}_{i+1} = \boldsymbol{\alpha}_i - \gamma_i \nabla_{\boldsymbol{\alpha}} \mathcal{Q}_i, \tag{6}$$

where γ_i is a scaling factor of the step length and $\mathcal{Q}$ is an approximation to the cost function. For energy minimization the cost function is simply the mean of the local energies over the set of configurations

$$\mathcal{Q} = \langle E_L \rangle = \frac{1}{m} \sum_{j=1}^{m} E_L(\mathbf{R}_j). \tag{7}$$

The scaling factor γ has an important role in averaging out the fluctuations in the approximate gradient, ensuring the convergence. On the other hand, too small a value of γ would overdamp the simulation. If one uses a sequence $\gamma_i \propto i^{-\beta}$, one should have $\frac{1}{2} < \beta \leqslant 1$.

Lin *et al.*[10] have shown that in the case of real wave functions and energy minimization, the derivative of the energy E with respect to a variational parameter α_i is simply

$$\frac{\partial E}{\partial \alpha_i} = 2\left\{ \left\langle E_L \times \frac{\partial \ln \Psi}{\partial \alpha_i} \right\rangle - E \times \left\langle \frac{\partial \ln \Psi}{\partial \alpha_i} \right\rangle \right\}, \tag{8}$$

where the average $\langle \cdots \rangle$ is over the whole Metropolis simulation.[10] One can implement this simple formula also for the SGA algorithm, with the small modification that the average is taken over only the current set of m configurations.

III. RESULTS

A. Comparison with other approaches

Before presenting the results for the Wigner-molecule-limit of a six-electron QD, we compare our VMC results with the most accurate QD results up-to-date. In a recent VMC and diffusion quantum Monte Carlo (DMC) study,[7] Pederiva *et al.* study quantum dots using a similar model as we do. They find the accuracy of VMC to be rather good compared to DMC, except in the case of three electrons. For this case, we have first taken the single-particle states to be the noninteracting ones with quantum numbers (0,0) and (1,0). With the GaAs choice of system parameters given above, the confinement energy corresponding to the study of Pederiva *et al.*[7] is around 3.32 meV. The total energy is found to be 26.563(1) meV (Ref. 11) which is reasonably close to the DMC value of Pederiva *et al.*, namely, 26.488(3) meV.[7] On the other hand, the VMC energy reported by Pederiva *et al.* is 29.669(3) meV.[7] Optimizing the exponentials lowers our VMC energy to 26.5406(8) meV. The difference of our VMC energy to the DMC one is around 0.05 meV which is small compared to the SDFT error ~ 0.4 meV.[7] For the six-electron case, the energy with noninteracting single-particle states is found to be 90.27(1) meV, which is again closer to the DMC energy 90.11(1) meV of Pederiva *et al.*[7] than the VMC one 90.368(4) meV. By freeing the parameters in the single particle states one does not lower the energy within the statistical error, and the optimal values are thus equal to the ones with the noninteracting states. This is a very important result, showing that the change in the wave function introduced by the Coulomb interaction is very accurately taken into account by the two-body Jastrow factors used. The reason why the optimization of the single-particle states was important in the three-electron case is most probably that there the number of spin-up and spin-down electrons is different.

TABLE I. Total energy (in meV) of the six-electron dot for different confinements and the two spin states.

	S=0		S=3	
$\hbar\omega$	VMC	ED[a]	VMC	ED[a]
7.576	168.90(1)	169.2	180.40(1)	180.5
2.678	76.91(1)	77.17	79.271(4)	79.38
1.458	49.101(5)	49.35	49.934(3)	50.10
0.947	35.864(3)	36.11	36.231(2)	36.41

[a]From Ref. 5.

It is also interesting to compare the results obtained with VMC with those of Reimann *et al.* for the six-electron case.[5] In their study, they use both SDFT and ED and consider six electrons with various strengths of the confining potential. We compare four different strengths of confinement, corresponding in their work to the cases of $r_s = 1$, 2, 3, and 4 a_B^*. Their ED energies are given in Table I with our VMC energies. One can see that the difference in the energies is between 0.1 and 0.3 meV, the VMC energies being lower. This comparison shows that the finite basis used by Reimann *et al.* is too restricted to describe the many-body wave function accurately. This comparison also shows that the results obtained with VMC are very accurate for the particle number in question.

We also compare the accuracy of our VMC results with the path-integral Monte Carlo simulations of Reusch *et al.* for $N = 8$.[8] As we are below mainly interested in the fully spin-polarized states, we compare only the $S = 4$ energies. This is not a closed-shell case, and our variational wave function for the two highest states is constructed from the four states with $n_x + n_y = 3$. For interaction strength $C = 2$,

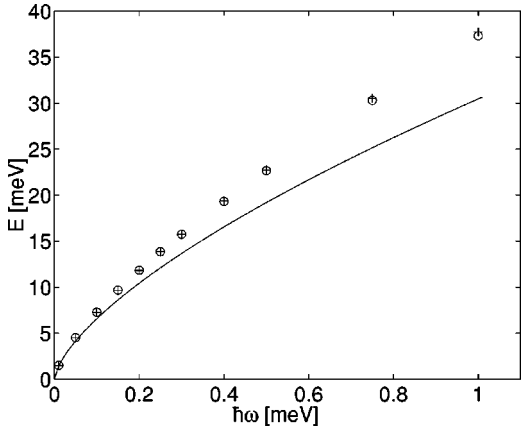

FIG. 1. Total energy for spin states $S=3$ (marked with pluses) and $S=0$ (circles) as a function of $\hbar\omega$. The line presents the classical energy $E_{\rm cl}^*$.

their energy is 48.3(2) $\hbar\omega$ which is slightly higher (but within error bars) than our energy of 48.201(1) $\hbar\omega$. As one can see, the statistical error is two orders of magnitude smaller in our result. For their most strongly interacting case, namely $C=8$, Reusch *et al.* obtain energy 103.26(5) $\hbar\omega$ which is again less accurate than our energy 103.137(1) $\hbar\omega$. Also this test shows that our results are very accurate in the limit of strong interaction.

One can conclude from these comparisons that the wave function used is very accurate. Most striking is the observation that after the Jastrow factor is added to the wave function, one can use the noninteracting single-particle states in the Slater determinants. Usually in VMC studies there is some ''residual'' interaction effects beyond Jastrow-approximation that are taken into account in a mean-field fashion by modified single-particle states in the Slater determinants.

B. Classical limit

Next, we study the transition to the classical limit in the six-electron case. The ground-state structure of six purely classical point charges in a parabolic potential minimizes the energy

$$E_{\rm cl}=\frac{1}{2}\sum_i r_i^2+\sum_{i<j}\frac{C}{r_{ij}}, \tag{9}$$

where we have used reduced units.[6] If we keep other parameters fixed and change only the confinement strength ω (as we do below), one can see that the interaction strength C scales as $C\propto\omega^{-1/2}$. The minimum-energy positions of electrons form a pentagon around one electron at the center. One can find the scaling of the classical cluster size and energy by writing the coordinates as $\mathbf{r}=r_c\hat{\mathbf{r}}$, where coordinates $\hat{r}$ are fixed and the scaling is in r_c. This results for the energy

$$E_{\rm cl}=r_c^2\frac{1}{2}\sum_i \hat{r}_i^2+\frac{C}{r_c}\sum_{i<j}\frac{1}{\hat{r}_{ij}}=r_c^2V_1+\frac{C}{r_c}V_2, \tag{10}$$

where V_1 and V_2 are constants, and solving $\partial E_{\rm cl}/\partial r_c=0$ results in $r_c=(CV_2/V_1)^{1/3}\propto\omega^{-1/6}$. Thus the energy scales

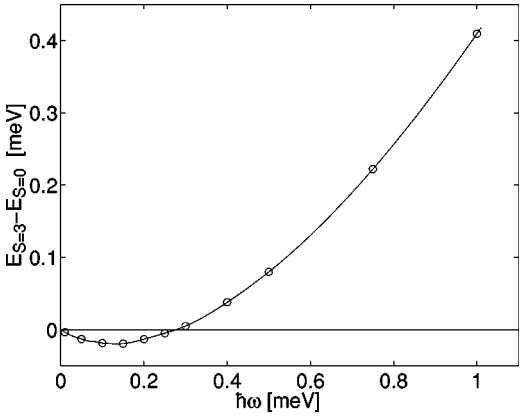

FIG. 2. Energy difference between the spin states $S=3$ and $S=0$ as a function of $\hbar\omega$. The line is to guide the eye.

(in units of ω) as $E_{\rm cl}\propto\omega^{-1/3}$. The minimum energy $E_{\rm cl}^*$ can be found to be $E_{\rm cl}^*[\text{meV}]\approx 30.46(\hbar\omega[\text{meV}])^{2/3}$.

The quantum-mechanical energies resulting from our VMC calculations for two spin polarizations are presented in Fig. 1 with the classical energy $E_{\rm cl}^*$. One can see that the quantum-mechanical energies are very close to each other, especially in the small $\hbar\omega$ limit, where the energies also approach the classical one. The difference between the quantum-mechanical energies can be seen more clearly in Fig. 2, where we have plotted the energy difference between the fully and nonpolarized states. One can see that spin polarization is predicted at $\hbar\omega\approx 0.28$ meV. We have not found ground states with partial spin polarization. Below, we concentrate on the fully spin-polarized case. If one subtracts from the total energy the minimum value of the classical potential energy $E_{\rm cl}^*$, the remaining energy has a linear behavior at small $\hbar\omega$ as shown in Fig. 3. One way of understanding this linear behavior is to consider first the limit $\hbar\omega\to 0$. In this limit, the electrons localize to the classical positions. If $\hbar\omega$ is now made larger, the electrons start to oscillate around the classical positions. A first approximation for this is to assume that each electron is in a harmonic potential $\tilde{V}(\mathbf{r}_i)=\frac{1}{2}\tilde{\omega}^2r_i^2$, with the strength scaling as $\tilde{\omega}\propto\omega$ as a function of ω. As a result of this, the total energy has, apart

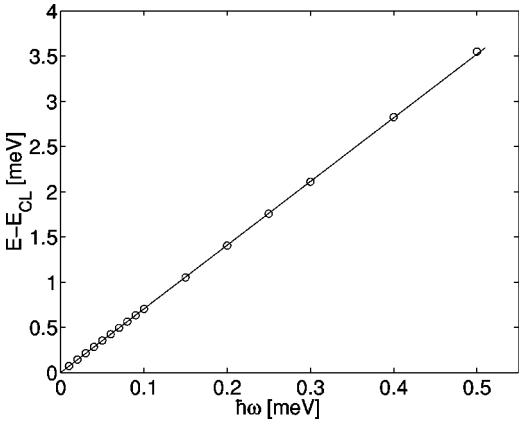

FIG. 3. Remaining energy for $S=3$ when $E_{\rm cl}^*$ (see text) is subtracted. The line presents a linear fit to points $\hbar\omega\leqslant 0.1$ meV.

from the classical energy, a zero-point energy that also scales as $\tilde{\omega}$. Thus we obtain a linear behavior for the difference between the total energy and the classical energy similarly as in Fig. 3. The error in the linear fit of Fig. 3 is smaller than 3 μeV for $\hbar\omega \leqslant 0.1$ meV where the fit is made, and for $\hbar\omega = 1$ meV still only 0.2 meV, which is of the same order as the difference in energy between the VMC and ED results in Table I. For $\hbar\omega = 2$ meV the error is around 1 meV. Thus the approximation derived above works surprisingly well even for a rather strong confinement. One should note that the approximation did not contain any information of the interaction between electrons (apart from the classical potential energy), and thus the system can be seen energetically as a collection of nearly independent electrons oscillating in an effective potential.

The most probable configuration $\mathbf{R}^*$, maximizing the density $|\Psi(\mathbf{R})|^2$ should approach in the limit of weak confinement the classical electron positions. This is not, however, enough to show that the system is close to a classical one. One can study the quantum fluctuations very conveniently using the conditional single-particle probability distribution $\tilde{\rho}(\mathbf{r})$, defined as

$$\tilde{\rho}(\mathbf{r}) = \left| \frac{\Psi(\mathbf{r}, \mathbf{r}_2^*, \ldots, \mathbf{r}_N^*)}{\Psi(\mathbf{r}_1^*, \mathbf{r}_2^*, \ldots, \mathbf{r}_N^*)} \right|^2, \tag{11}$$

where the coordinates $\mathbf{r}_i^*$ are fixed to the ones from the most probable configuration $\mathbf{R}^*$. In the classical limit, the density $\tilde{\rho}(\mathbf{r})$ is more and more peaked around the classical position $\mathbf{r}_1^*$, but still shows quantum fluctuations. For the two-electron case, this is very similar to the conditional probability distribution used for a two-electron QD.[12] One difference is that in $\tilde{\rho}$ the fixed electron is at the most probable position, which is in our opinion the most natural choice. The most important advantage of $\tilde{\rho}$ is that it shows much more clearly the amount of localization for larger particle numbers than the conditional probability distribution. The reason for this is that one usually fixes only one electron in constructing the conditional probability distribution, and when the particle number is large, the effect of one fixed electron gets smaller, and the rest of the electrons can, for example, show collective motion that conceals the localization. If, on the other hand, one fixes all but one electron, the most natural choice is $\tilde{\rho}$. The calculation of $\tilde{\rho}$ is very easy, especially in VMC. One should first, of course, find the most probable electron positions. In doing this, the gradient of the wave function (needed also for the calculation of the local energy, and for this reason usually done analytically) is very useful. After that, one moves the ''probe electron'' to all points where the value of $\tilde{\rho}$ is wanted, and evaluates the ratio of wave functions as in Eq. (11). This ratio is automatically done when sampling the configurations in a VMC simulation. One should also notice that $\tilde{\rho}$ does not contain noise unlike many more common VMC observables, such as the density or the radial pair distribution function.

In Fig. 4 we show $\tilde{\rho}$ for four different confinement strengths from 10 to 0.01 meV. The most probable electron positions are for all strengths similar to the classical ones with one electron in the center of a pentagon. The quantum effects make the most probable coordinates slightly larger than the classical ones, but the difference vanishes for weak confinement. One can also see that $\tilde{\rho}$ is more localized for weaker confinement, but only the one with $\hbar\omega = 0.01$ meV looks like a Wigner molecule. In that case, all the points on the line $\tilde{\rho} = 0.01$ are closer to $\mathbf{r}_1^*$ than any other $\mathbf{r}_i^*$. Also the snapshot animations of the systems during the simulations[13] show the case of $\hbar\omega = 0.01$ meV to resemble what one expects for a Wigner molecule. As we work with a finite system, we do not have a real phase transition between $\hbar\omega = 0.1$ and 0.01 meV. In a two-dimensional electron gas, the phase transition to a Wigner crystal has been suggested to happen at the density $r_s \approx 37 \pm 5$ (Ref. 14) (in units of effective Bohr radius a_B^*, which is around 9.79 nm for our system parameters). The radius of a circle that encloses one electron on the average is thus around 360 nm at the transition point. This is in a good agreement with the interelectron distances shown in Fig. 4, since in Fig. 4(c) the distance of edge electrons to the center one is smaller than the suggested critical 360 nm, and in Fig. 4(d) the distance is roughly four times the critical one. The approximative relation between r_s and $\hbar\omega$ presented in Ref. 5 gives $\hbar\omega \approx 0.034$ meV for $r_s = 37$, which is nicely between the cases of Figs. 4(c) and 4(d).

It is also interesting to see the similarity between the effective single-particle potentials $\tilde{V}$ shown in Figs. 5(a) and 5(b), and the corresponding $\tilde{\rho}$ in Figs. 4(c) and 4(d). This similarity could be used to describe the system, as we did above, as a system of six independent electrons, each with its own effective potential $\tilde{V}$. The assumption of parabolic $\tilde{V}$ could easily be replaced by, e.g., $\tilde{V} = \frac{1}{2}(\tilde{\omega}_{x,i}^2 x_i^2 + \tilde{\omega}_{y,i}^2 y_i^2)$ keeping the problem still solvable. There are, however, contributions that are not taken into account in this simple model, such as the exchange energy which is important for the spin polarization of the system. Another aspect of the similarity between $\tilde{\rho}$ and $\tilde{V}$ is that it draws a connection between the wave function and the potential in a similar fashion that is often assumed in a semiclassical approximation. This could be used to motivate the studies of classical charged particles in various confinements and also a semiclassical approach in the limit where the electrons are close to forming a Wigner molecule.

The transition to a Wigner-molecule-like regime can also be seen in the radial pair distribution function, shown in Fig. 6. The function is clearly more peaked for weaker confinement. The peak at $r = 1$ consists of two types of electron pairs, namely, ones with both electrons on the edge, and ones with an electron in the center and the other on the edge. The electron-electron distance in the pair of the first type is in a classical solution 18% longer than in the second, the number of different pairs being the same in the classical solution. This double nature cannot be seen in the first peak of $g(r)$. This is not surprising, as particle exchanges happen even with $\hbar\omega = 0.01$ meV.[13] To study exchange, we have followed the most probable electron positions while forcing the electron originally in the center to move to the edge. The symmetry is broken by making small random displacements

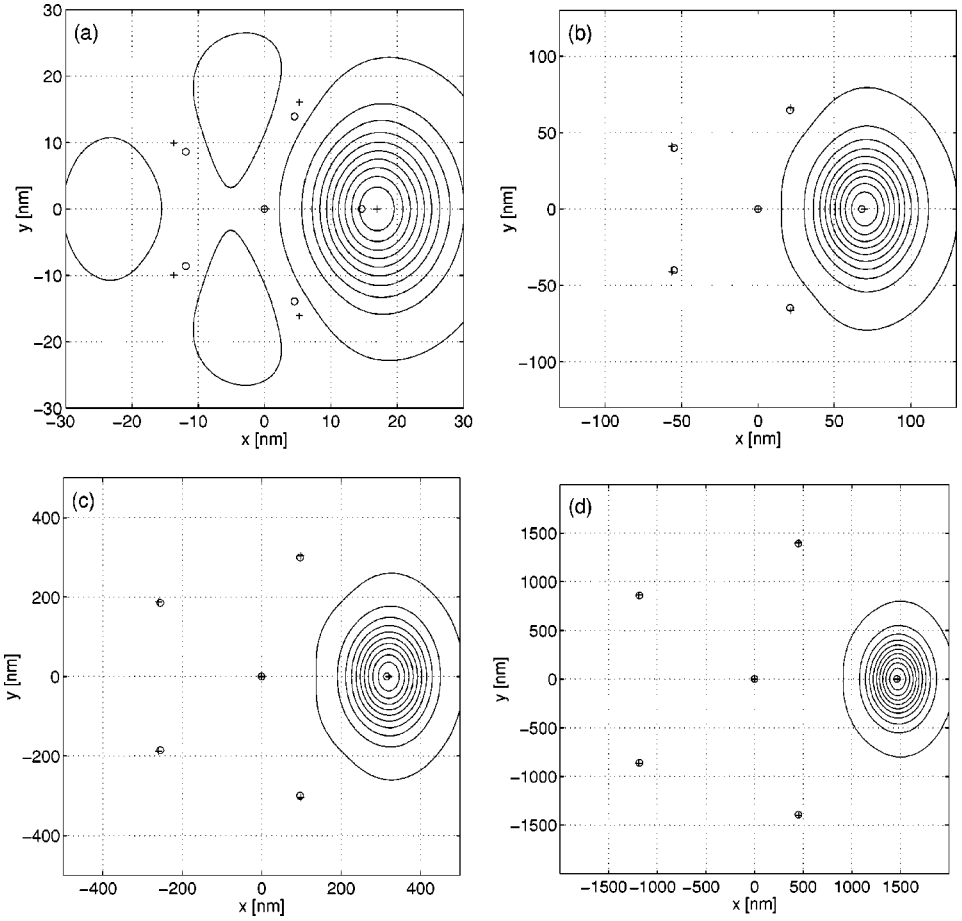

FIG. 4. Conditional probability density $\tilde{\rho}(\mathbf{r})$ for the right-most electron. The contours are uniformly from 0.01 to 0.91. We mark with a plus the most probable electron positions, and with a circle the classical positions. The confinement strength $\hbar\omega$ is (a) 10 meV, (b) 1 meV, (c) 0.1 meV, and (d) 0.01 meV.

of the electrons. The particle exchange involves three or more electrons, as shown in Fig. 7. One can see a collective rotation of the edge electrons before one is moved halfway to the edge. This kind of exchange is very easy for the small QD's as the one in question. One could argue that larger electron numbers would make the multiparticle exchanges a more unlikely process.

Compared with the experimental realizations of GaAs QD's, the electron density where the Wigner molecule is found is extremely small. We feel that impurities would move the transition to larger densities as in the 2D electron gas, where the transition is found to move to $r_s \approx 7.5\ a_B^*$.[15] For this, the approximative relation[5] gives $\hbar\omega \approx 0.37$ meV, which is already closer to the typical confinement strengths in experiments. It would also be very interesting to study the effect of impurities on the spin polarization transition.

IV. SUMMARY AND CONCLUSIONS

We have first shown that the VMC method results in energies in good agreement with the most accurate results available. In VMC, the construction of the wave function clearly plays a central role. We have shown that the efficiency of SGA allows us to carefully optimize also the

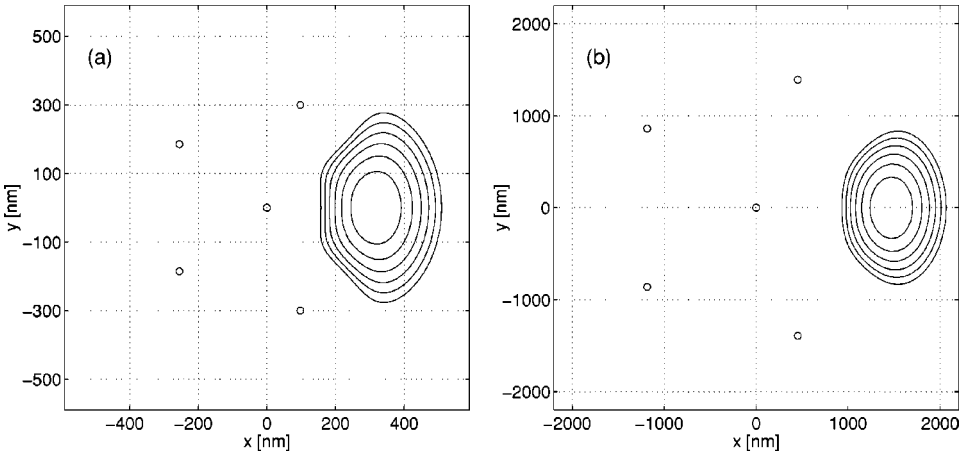

FIG. 5. Potentials felt by one of the electrons (contours uniformly from half to three) when the five other electrons are on their classical positions (marked with a circle). The confinement strength $\hbar\omega$ is (a) 0.1 meV and (b) 0.01 meV.

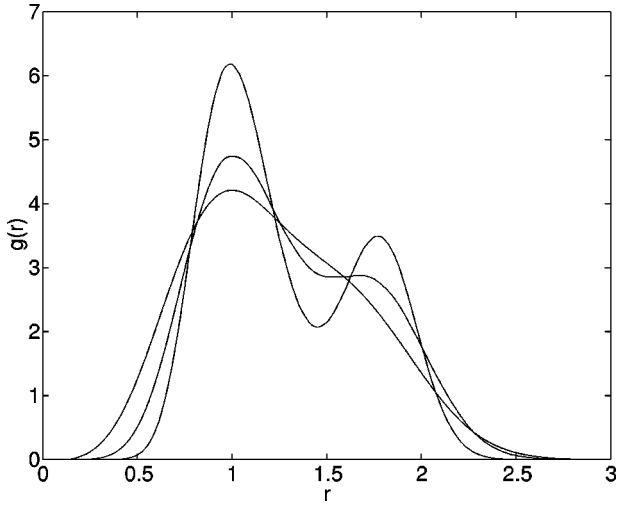

FIG. 6. Radial pair distribution function for $\hbar\omega = 1.0$, 0.1, 0.01 meV. The curves with smaller $\hbar\omega$ are more peaked. r is scaled to set the first peak to one.

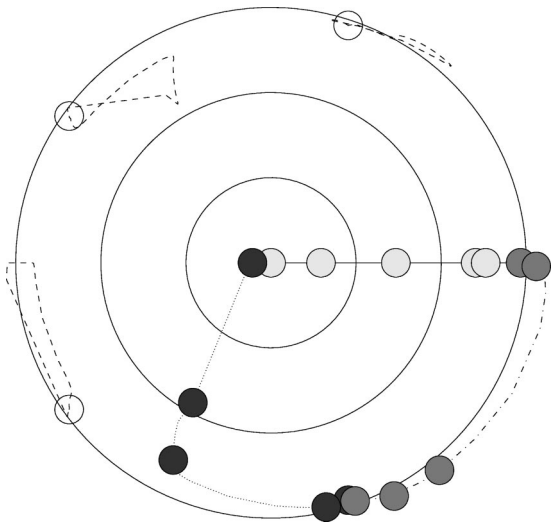

FIG. 7. Particle exchange for $\hbar\omega = 0.01$ meV. The electron from the center (marked with light-gray circle) is moved to the right along the solid line. The rest of the electrons are always at their most probable positions. For the electrons ending at the starting position, only these positions and the path followed is shown. The circles showing the distance from the center have a radius from 500 to 1500 nm.

single-particle part of the wave function, resulting in VMC energies more accurate than the previous ones where the single-particle states are taken from a mean-field approach.[7] On the other hand, our results show that in many cases the noninteracting single-particle states are optimal or very close to the optimal ones. This is probably related to the high symmetry of the parabolic QD and the separation of the center-of-mass and relative motion. We feel that the efficiency of the SGA method would be even more useful in low-symmetry dots.

Unlike in the previous accurate study of the six-electron QD,[5] we have been able to reach low enough densities to find a spin polarization of electrons and, in an even lower density, a smooth transition to a Wigner-molecule-like state. The transition happens roughly at the same density as in the 2D electron gas.[14] One should note that the 2D electron gas does not spin polarize before the transition to a Wigner crystal, but the spin polarized state is very close in energy.[14] One possible explanation for the difference could be that the multiparticle exchange we find in the six-electron dot favors spin polarization. In the 2D electron gas, such a process is less favorable. To qualitatively study the transition to a Wigner-molecule-like state, we have introduced a measure function $\tilde{\rho}$, which we show to be very useful for the study of the electron localization.

Overall, we have found VMC to be a perfect tool for studying the properties of QD's in a wide range of system parameters, resulting in energies in good agreement with the most accurate results available and enabling us to study the delicate transition of a QD to the classical regime.

ACKNOWLEDGMENTS

We would like to thank M. Alatalo, M. Marlo, H. Saarikoski, and V.A. Sverdlov for useful discussions and comments. This research has been supported by the Academy of Finland through its Centers of Excellence Program (2000–2005).

[1] L.P. Kouwenhoven and C.M. Marcus, Phys. World **11**, 35 (1998).
[2] L.P. Kouwenhoven, T.H. Oosterkamp, M.W.S. Danoesastro, M. Eto, D.G. Austing, T. Honda, and S. Tarucha, Science **278**, 1788 (1997).
[3] A. Harju, V.A. Sverdlov, R.M. Nieminen, and V. Halonen, Phys. Rev. B **59**, 5622 (1999).
[4] A. Harju, S. Siljamäki, and R.M. Nieminen, Phys. Rev. B **60**, 1807 (1999).
[5] S.M. Reimann, M. Koskinen, and M. Manninen, Phys. Rev. B **62**, 8108 (2000).
[6] We measure the length in units of $l_0 = \sqrt{\hbar/m^*\omega}$. The scaled strength of the Coulomb interaction is $C = \sqrt{\mathrm{Ha}/\hbar\omega}\sqrt{m^*/m_0}/\epsilon$, where Ha is Hartree.
[7] F. Pederiva, C.J. Umrigar, and E. Lipparini, Phys. Rev. B **62**, 8120 (2000).
[8] B. Reusch, W. Häusler, and H. Grabert, Phys. Rev. B **63**, 113313 (2001).
[9] A. Harju, B. Barbiellini, S. Siljamäki, R.M. Nieminen, and G. Ortiz, Phys. Rev. Lett. **79**, 1173 (1997).
[10] X. Lin, H. Zhang, and A.M. Rappe, J. Chem. Phys. **112**, 2650 (2000).
[11] The numbers in the parentheses are the statistical uncertainties in the last digit.
[12] C. Yannouleas and U. Landman, Phys. Rev. B **61**, 15 895 (2000).
[13] Animations for various systems can be found from URL http://www.fyslab.hut.fi/arch/aph/cl_qd.html
[14] B. Tanatar and D.M. Ceperley, Phys. Rev. B **39**, 5005 (1989)
[15] S.T. Chui and B. Tanatar, Phys. Rev. Lett. **74**, 458 (1995).